Design and calibration of unicapillary pneumotachographs

A. Giannella-Neto, C. Bellido, R. B. Barbosa and M. F. Vidal Melo

J Appl Physiol 84:335-343, 1998. ;

Journal of Applied Physiology publishes original papers that deal with diverse area of research in applied physiology, especially those papers emphasizing adaptive and integrative mechanisms. It is published 12 times a year (monthly) by the American Physiological Society, 9650 Rockville Pike, Bethesda MD 20814-3991. ISSN: 8750-7587, ESSN: 1522-1601. Visit our website at http://www.the-aps.org/.

Design and calibration of unicapillary pneumotachographs

A. GIANNELLA-NETO, C. BELLIDO, R. B. BARBOSA, AND M. F. VIDAL MELO
Biomedical Engineering Program, Graduate School of Engineering, Federal University of Rio de Janeiro, Rio de Janeiro, Brazil, 21945-970

Giannella-Neto, A., C. Bellido, R. B. Barbosa, and M. F. Vidal Melo. Design and calibration of unicapillary pneumotachographs. *J. Appl. Physiol.* 84(1): 335–343, 1998.—This study presents a method for design and calibration of unicapillary pneumotachographs for small-animal experiments. The design, based on Poiseuille's law, defines a set of internal radius and length values that allows for laminar flow, measurable pressure differences, and minimal interference with animal's respiratory mechanics and gas exchange. A third-order polynomial calibration (Pol) of the pressure-flow relationship was employed and compared with linear calibration (Lin). Tests were done for conditions of ambient pressure (Pam) and positive pressure (Ppos) ventilation at different flow ranges. A physical model designed to match normal and low compliance in rats was used. At normal compliance, Pol provided lower errors than Lin for mixed (1–12 ml/s), mean (4–10 ml/s), and high (8–12 ml/s) flow rate calibrations for both Pam and Ppos inspiratory tests ($P < 0.001$ for all conditions) and expiratory tests ($P < 0.001$ for all conditions). At low compliance, they differed significantly with 8.6 ± 4.1% underestimation when Lin at Pam was used in Ppos tests. Ppos calibration, preferably in combination with Pol, should be used in this case to minimize errors (Pol = 0.8 ± 0.5%, Lin = 6.5 ± 4.0%, $P < 0.0005$). Nonlinear calibration may be useful for improvement of flow and volume measurements in small animals during both Pam and Ppos ventilation.

small animals; flow and volume measurement; mechanical ventilation; physical model

SMALL ANIMALS are intensively used in experimental medicine due to availability, easy manipulation, and the economic, ethical, political, and social pressures against the use of larger animals. In relation to the respiratory system (RS), this trend leads to measurement challenges because some physiological variables like tidal volume (V_T) can be reduced up to 1,000-fold compared with human values.

One of the most frequently used techniques for assessment of ventilatory flows and volumes is pneumotachography (7, 12, 15). Pneumotachographs, either directly connected to the respiratory tubing or attached to a body plethysmograph, can be used in small-animal experiments. Technical characteristics such as accuracy, sensitivity, linearity, frequency response, low resistance, and low dead space make these instruments practical for studies in small animals. Glass et al. (9) proposed a face mask and Fleisch head, which can be regarded as a unicapillary pneumotachograph, for studies during rest or activity in amphibians, reptiles, and birds. Mortola and Noworaj (13) presented a study of two-sidearm tracheal cannulas to be used in mammals weighing 15–350 g. Four sizes were proposed, and the device consisted essentially of a cannula with two lateral ports for differential pressure measurements. Marano (11), working with rats and guinea pigs, proposed a traditional solution of summing the separate flows measured on the inflation and deflation limbs of the breathing circuit by using two pneumotachographs, to reduce the added dead space represented by a single pneumotachograph to measure both inspired and expired volumes. Schuessler et al. (18) and Schuessler and Bates (17) developed an ingenious computer-controlled ventilator for small animals and substituted the pneumotachograph by measuring the position of a piston and the pressure inside the ventilator's rigid cylinder. Their results were also very accurate for higher frequencies. However, complex instrumentation was necessary, and only inspiratory flow measurements were available for small animals under mechanical ventilation.

The geometry of generally used experimental respiratory arrangements can cause different flow patterns, and thus distinct calibration coefficients, during inspiration and expiration (6). In addition, arrangement of the tubes, unsteady flow, abrupt changes in luminal diameter, sharp edges, sudden changes in the direction of flow, and high flow rates can produce nonlinearities related to turbulence (1). A method for nonlinear calibration of the Fleisch no. 3 pneumotachograph has been proposed that allowed for improved results of pneumotachograph-based spirometers when evaluated according to American Thoracic Society standards compared with linear approaches (8). In the case of mechanically ventilated animals, factors related to positive pressure ventilation (Ppos) in the system are added. Thus use of unicapillary pneumotachographs as proposed for small animals of different species (9, 13) in situations such as rest, exercise, or mechanical ventilation leads to the need for designing and calibrating the device in specific conditions. However, criteria for design and calibration of the unicapillary pneumotachograph in different experimental settings are still undefined.

In the present study, criteria for construction of a unicapillary pneumotachograph for small-animal experiments useful for inspiratory and expiratory flow measurements are presented, and an evaluation of linear and nonlinear calibrations is performed for the case of ambient pressure (Pam; spontaneous ventilation) and Ppos ventilation.

MATERIALS AND METHODS

Glossary

α_R	Fraction of respiratory system resistance allowable in the pneumotachograph
α_V	Fraction of tidal volume allowable in the pneumotachograph
ΔP	Differential pressure measured in the side ports of pneumotachograph

ΔP_{min}	Minimal measurable differential pressure
η	Dynamic viscosity
ρ	Fluid density
C	Animal's respiratory system compliance
D	Internal diameter of the tube or pneumotachograph
L	Length between pneumotachograph differential pressure measuring ports
L_{tot}	Total pneumotachograph length
P_B	Barometric pressure
r	Internal radius of the tube or pneumotachograph
Re	Reynolds number
Rpt	Pneumotachograph resistance
Rrs	Animal's respiratory system resistance
V	Internal volume of the physical model
v_{max}	Maximal velocity
$\dot{V}_{max}$	Maximal flow rate
$\dot{V}_{min}$	Minimal flow rate
Vpt	Pneumotachograph volume

International system units (SI) were used for formulation and computation. Results are presented in commonly used units.

Design of a Pneumotachograph

The construction of a unicapillary pneumotachograph can be based on four criteria: *1*) laminar flow, *2*) measurable differential pressures, *3*) minimal interference with respiratory mechanics, and *4*) minimal dead space. These criteria lead to a system of inequalities in the pneumotachograph dimensions length (L) and internal radius (r) that defines an area in the r vs. L plane to be used in the construction of the pneumotachograph.

Laminar flow. A linear relationship between pressure drop and flow is assumed to exist, and thus Poiseuille's law to be valid, in pneumotachographic measurements. This implies the existence of a laminar flow. For this, Re should be low

$$\mathrm{Re} = \frac{v_{max} \cdot D \cdot \rho}{\eta} \leq 2{,}000 \qquad (1)$$

Because

$$v_{max} = \frac{\dot{V}_{max}}{\pi \cdot r^2} \qquad (2)$$

a condition for minimal r is met

$$r \geq \frac{\dot{V}_{max} \cdot \rho}{1{,}000 \cdot \pi \cdot \eta} \qquad (3)$$

Measurable differential pressure. The values of pressure drops at the minimal flows should lead to measurable values for usual differential pressure transducers. The minimal measurable differential pressure (ΔP_{min}) is a characteristic of the pressure transducer, electronics, and the analog-to-digital converter system. It can be estimated as the pressure corresponding to twice the SD of the differential pressure baseline noise (16). The absolute flow rate corresponding to ΔP_{min} is the minimal measurable absolute flow rate ($\dot{V}_{min}$). By using Poiseuille's law

$$\Delta P = \frac{8 \cdot \eta \cdot L \cdot \dot{V}_{min}}{\pi \cdot r^4} \geq \Delta P_{min} \qquad (4)$$

Rearranging, a condition for maximal r is found

$$r \leq \sqrt[4]{\frac{8 \cdot \eta \cdot L \cdot \dot{V}_{min}}{\pi \cdot \Delta P_{min}}} \qquad (5)$$

Minimal interference with respiratory mechanics. This condition is introduced in the form of a fraction of the respiratory resistance that can be accepted to be present in the pneumotachograph

$$\mathrm{Rpt} \leq \alpha_R \cdot \mathrm{Rrs} \qquad (6)$$

By using Poiseuille's law to express the pneumotachograph resistance

$$\mathrm{Rpt} = \frac{8 \cdot \eta \cdot L_{tot}}{\pi \cdot r^4} \qquad (7)$$

and another condition for minimal r is established

$$r \geq \sqrt[4]{\frac{8 \cdot \eta \cdot L_{tot}}{\alpha_R \cdot \pi \cdot \mathrm{Rrs}}} \qquad (8)$$

Minimal dead space. The pneumotachograph dead space should be lower than a fraction of the animal's V_T

$$\mathrm{Vpt} = \pi \cdot r^2 \cdot L_{tot} \leq \alpha_V \cdot V_T \qquad (9)$$

and a further condition for maximal r is defined

$$r \leq \sqrt{\frac{\alpha_V \cdot V_T}{\pi \cdot L_{tot}}} \qquad (10)$$

The set of four inequalities (3, 5, 8, and 10) establishes a design region in the r vs. L plane that allows for the definition of pneumotachograph dimensions.

In consideration of the design for rats ventilated with ambient air, the following values were used in the present study.

$\rho = 1.176\ \mathrm{kg/m^{-3}}$
$\eta = 1.839 \cdot 10^{-5}\ \mathrm{N \cdot s \cdot m^{-2}}$
$\dot{V}_{max} = 12.0\ \mathrm{ml/s}$
$\dot{V}_{min} = 0.1\ \mathrm{ml/s}$
$V_T = 2.0\ \mathrm{ml}$
$\mathrm{Rrs} = 0.24\ \mathrm{cmH_2O \cdot s \cdot ml^{-1}} \approx 0.24 \times 10^8\ \mathrm{kg \cdot m^{-4} \cdot s}$
$\alpha_R = 0.2$
$\alpha_V = 0.1$
$\Delta P_{min} = 0.1\ \mathrm{Pa}$
$L_{tot}/L = 4.0.$

The pneumotachograph designed with use of these criteria was fashioned in polyvinyl chloride and used in the calibration procedures described below. To reduce dead space and connections, the inspiratory-expiratory Y piece was built in the same body of the pneumotachograph.

Construction of an RS Model

A physical model matching animal respiratory mechanics (for both compliance and resistance) was needed for experiments related to Ppos ventilation (Fig. 1A). Because no standards are set for construction of lung mechanics models

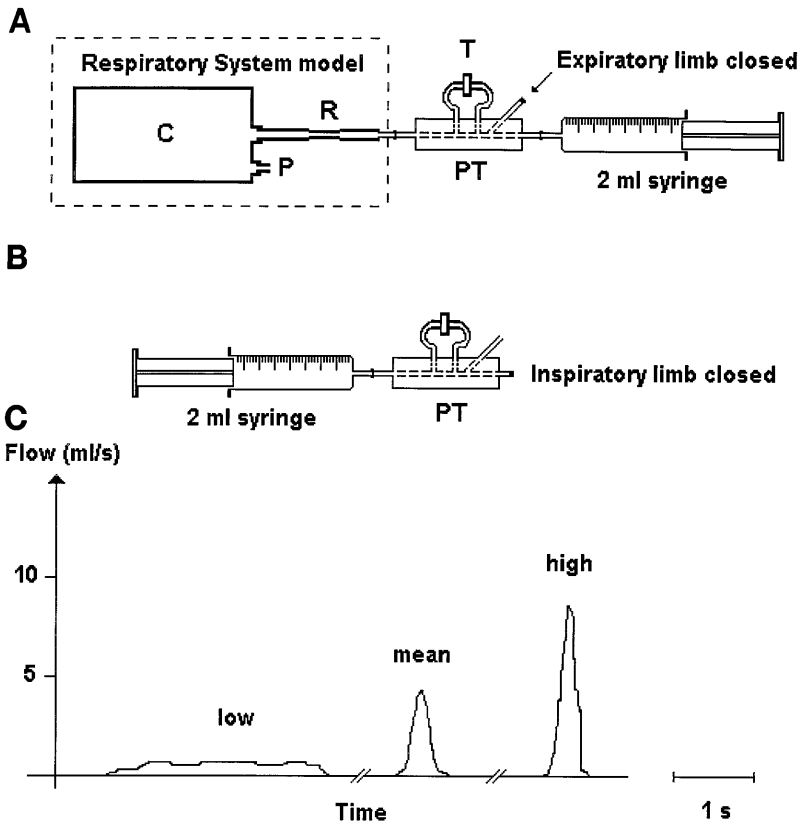

Fig. 1. Schematic experimental setup of calibration and tests in inspiration (*A*) and expiration (*B*) showing typical flow waveforms (*C*). C, compliance; R, resistance; P, port; T, pressure transducer; PT, pneumotachograph. Port is either closed (positive pressure; Ppos) or opened (ambient pressure; Pam).

for small animals, the criteria proposed by ISO 5369/87 (19) for human lung models were adapted to the present case.

Essentially, a vessel with rigid walls is used as the RS model compliance. Its internal volume is computed to match the desired compliance through the compressibility of the gas in the model. In consideration of perfect gas and isothermic conditions, this volume can be computed by using Boyle's law

$$V = C \cdot P_B \qquad (11)$$

To approximate isothermic conditions and thus minimize pressure changes due to temperature increase during air compression in the physical model, a heat absorber (copper wire wool, diameter = 0.045 mm), corresponding to 2% of internal volume, was placed in the model. Evaluation of isothermic conditions was done through pressure measurements in the closed system. Pressure was measured with a differential pressure transducer (Microswitch 163SC01D48, cutoff frequency >14 Hz). Five high-flow and five low-flow injections of 2.00-ml volumes were performed, and the ratio of the differences between peak to plateau pressure and peak to preinjection pressure was computed for each test.

The normal RS compliance was assumed to be equal to 0.57 ± 0.03 ml/cmH_2O, the value in rats according to Lai and Hildebrandt (10). The model was built as an aluminum cylinder with a 625-ml internal volume, corresponding to a compliance of 0.59 ml/cmH_2O after insertion of copper wool. To simulate low-compliance conditions, aluminum cylinders were introduced in the model, reducing the internal volume to 78 ml. Similarly to the first case, copper wool was inserted, resulting in 0.074 ml/cmH_2O equivalent compliance. Normal compliance was experimentally evaluated by plotting a pressure-volume curve of the model by using a calibrated syringe and a pressure transducer (Calibration Analyzer, RT-200 Allied Healthcare Products). Low compliance was measured during the test for isothermia, where the injected volume (2.00 ml) was divided by the plateau pressure.

Lung resistance was constructed with a needle syringe (internal diameter = 0.80 mm, length = 18 mm) to simulate a laminar flow resistance of 0.26 cm$H_2O \cdot ml^{-1} \cdot s$, which represents a normal value in rats (2). The resistance was tested by measuring the differential pressure drop for a flow rate equal to 2 ml/s and resulted in a value equal to 0.21 cm$H_2O \cdot ml^{-1} \cdot s$. The sharp end of the needle was connected externally to the vessel with a short tube. The vessel was provided with a second orifice, normally occluded. This port was opened when Pam calibrations and tests were performed (see below).

Pneumotachograph Calibration and Tests

Calibrated syringes containing 2.00 and 5.00 ml were used in the procedure. All tests were performed in ambient temperature room air, and the pneumotachograph was not heated. The unicapillary pneumotachograph was connected to a differential pressure transducer [Celesco, model low-cost variable reluctance (LCVR), pressure range 0–2 cmH_2O] by short tubes (length = 10 cm, internal diameter = 4 mm). Appropriate electronic amplification and filtering (30 Hz, first order low pass) was performed. Signals were sampled at 100 Hz with use of a 12-bit analog-to-digital converter coupled to an IBM-PC-compatible microcomputer.

The set of calibration curves was constructed from manually driven injections. During inspiratory calibration, the syringe was connected to the inspiratory limb of the respiratory circuit, with the expiratory limb occluded (Fig. 1*A*). The opposite side of the pneumotachograph was then connected to the RS model. For expiratory calibration, the model has been substituted by the syringe in the respiratory circuit and the inspiratory limb was occluded (Fig. 1*B*); in this situation, the model was not used because the RS impedance would

limit the frequency content of expiratory waveforms. Each set of calibrations consisted of six syringe injections and was designated, according to the mean flow rates of its curves, as low (1–6 ml/s), mean (4–10 ml/s), or high (8–12 ml/s). Injection times were selected to equally distribute mean flow rates. These were computed as injected volume divided by injection time, calculated automatically by the calibration software. Global calibration (mixed; 1–12 ml/s) combined the three sets previously defined, making a total of 18 injections. In all calibration conditions, low-, mean-, high-, and mixed-flow rate injections were considered. The calibration curves were either a straight line or a third-order polynomial fitted to the calibration points, according to a minimal mean square error procedure (see APPENDIX).

The following calibration conditions were studied.

Inspiratory normal-compliance calibrations: Pam (open physical model) and Ppos (closed physical model) conditions. These correspond, respectively, to a resistive and a resistive plus normal-compliance load. Injected volumes were 2.00 and 5.00 ml, corresponding to 3.4 and 8.5 cmH_2O final pressure under Ppos conditions, respectively.

Inspiratory low-compliance calibrations: Pam and Ppos conditions. These correspond to a resistive and resistive plus low-compliance load. Injected volume is equal to 2.00 ml (final pressure = 27.0 cmH_2O).

Expiratory calibrations. Injected volumes were 2.00 and 5.00 ml.

Tests for all described calibrations consisted of 50 consecutive injections randomly selected among low, mean, or high flow rates. The same loads used during calibrations were employed. Tests were done immediately after the correspondent calibration, to maintain equivalent ambient conditions. Ambient temperature, humidity, and Pam during experiments ranged from 18 to 24°C, 64 to 76%, and 759 to 770 mmHg, respectively.

Statistics

Errors were expressed as percent errors and their absolute values. Analysis of variance was used to compare errors obtained from linear and third-order polynomial calibrations by using different mean-flow rate profiles. Statistical significance was set at $P < 0.05$.

RESULTS

Pneumotachograph Design

Figure 2 displays a plot of the pneumotachograph *r* vs. *L* plane for design conditions. Areas are limited by curves, corresponding to inequalities (3, 5, 8, and 10). The design region is identified by the hatched area. The pneumotachograph used in the experiments was built according to the dimensions defined by that region, with an 1.8-mm internal diameter, a total length of 60.0 mm, and 15.0 mm between pressure-measuring ports (Fig. 3).

RS Model

An experimental compliance curve was built for the normal-compliance condition. Volume and pressure were linearly related with use of the equation $V = (0.613 \pm 0.006) \cdot P - (0.061 \pm 0.066)$ ($P < 0.001$). Such values can be compared with the theoretical values equal to $V = 0.59 \cdot P$. The mean error percent between measured and computed pressures was 1.0%. Low compliance measured 0.0770 ± 0.0003 ml/cmH_2O (theoretical = 0.074 ml/cmH_2O).

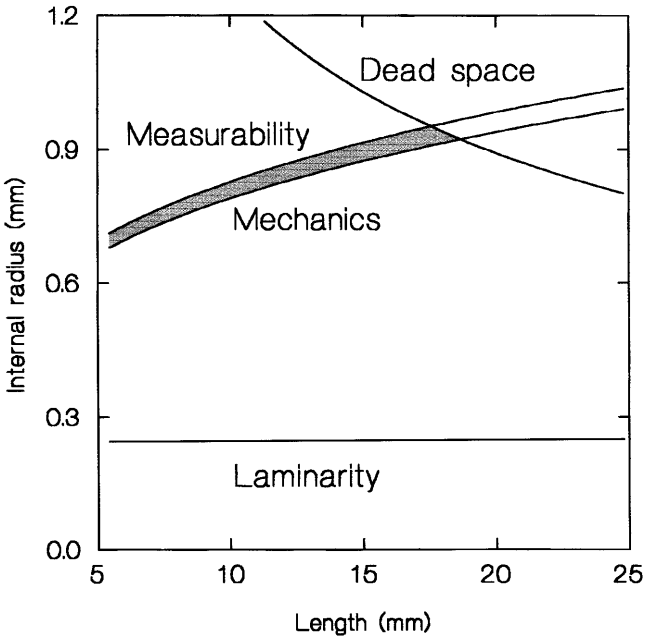

Fig. 2. Design curves on pneumotachograph internal radius vs. length between side ports plane. Shaded area is design region and is limited above by curve defined by measurability criteria and below by curve of minimal interference with lung mechanics. Lines corresponding to maximal dead space and laminarity criteria are also indicated.

Mean ratios of differences between peak to plateau pressure and peak to preinjection pressure after high- and low-flow injections in the normal- and low-compliance models were computed. For both models, no differences were found between peak and plateau pressures for low-flow injections. For high flows, noticeable differences ranging from 3.1 to 3.8% (5 tests) were found only in the low-compliance situation.

Pneumotachograph Calibration

Figure 4 presents both the linear and the polynomial inspiratory calibration curves representing the calibration under Pam conditions by using a syringe volume of

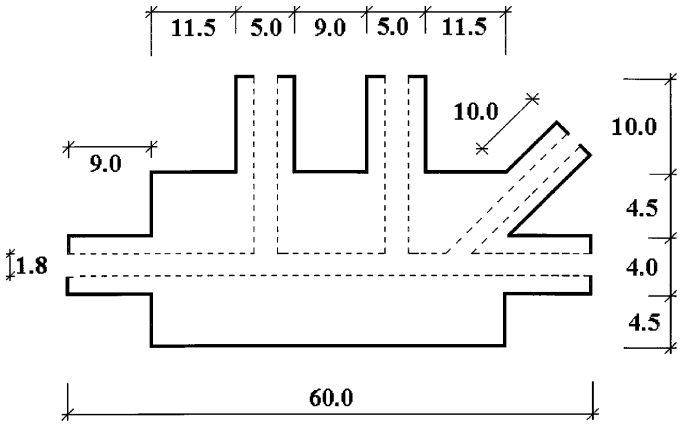

Fig. 3. Scheme of constructed unicapillary pneumotachograph. Figure is not in scale. Inclined branch refers to expiratory path. Units are in millimeters.

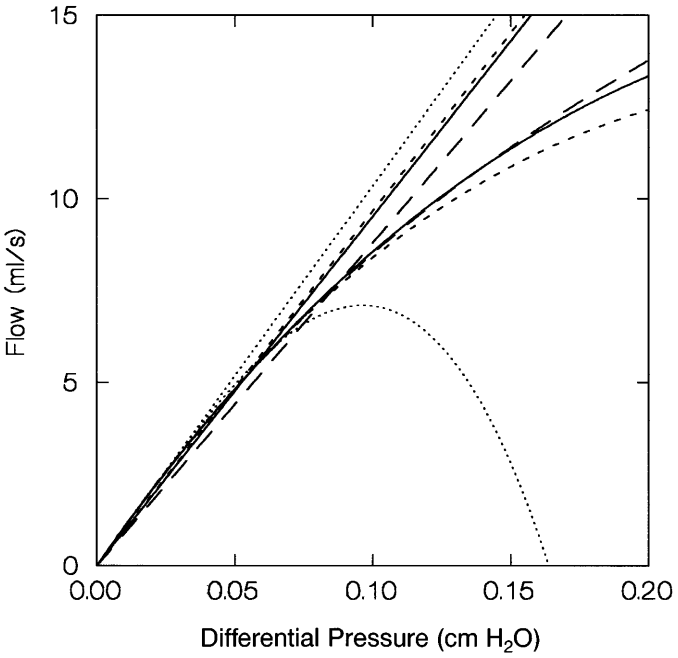

Fig. 4. Linear and third-order polynomial inspiratory calibration curves under Pam conditions for low (dotted lines), mean (long dashed lines), high (short dashed lines), and mixed (solid lines) flow rates. Injected volume, 2.00 ml.

2.00 ml and the normal-compliance model. In this case, substituting the normal- for the low-compliance model resulted in essentially the same calibration curves. It is noteworthy that linear and polynomial calibrations are roughly superimposed only for very low flow rates. Also, for the polynomial calibration the low-flow calibration curve markedly diverges from the others at flows >7 ml/s. Calibration curves for the Ppos condition with injection volumes equal to 2.00 and 5.00 ml in the same setting essentially overlapped those for the Pam condition.

Table 1 presents the error percents for 50 injections with the 2.00-ml syringe and mean flows in the range from 1 to 12 ml/s for inspiration by using the normal-compliance RS model (Pam and Ppos) and expiration. Volumes were computed with different calibrations curves. Means of absolute error percents for calibration based on low, mean, high, and mixed flows as well as linear and nonlinear calibrations are presented. Lowest error percents for both inspiratory and expiratory tests were obtained for nonlinear calibration by using high (inspiratory, Ppos: polynomial = 1.1 ± 0.9 vs. linear = 9.9 ± 5.1, $P < 0.001$; expiratory: polynomial = 1.0 ± 0.8 vs. linear = 4.0 ± 2.1, $P < 0.001$) or mixed (inspiratory, Ppos: polynomial = 0.9 ± 0.7 vs. linear = 8.2 ± 5.0, $P < 0.001$; expiratory: polynomial = 0.8 ± 0.5 vs. linear = 2.8 ± 1.9, $P < 0.001$) flows. However, very high error percents (16.2 ± 21.0) were obtained with the nonlinear calibration when the curve was based only on low flows.

Dependence of error on mean flow rates is shown in Fig. 5 for linear and nonlinear calibration based on mixed flows for inspiratory tests performed in both RS models at Ppos. Fifty injections were done for each

Table 1. *Errors in volume measurements according to curve fitting, mean-flow range, and pressure condition during calibration by using normal-compliance physical model*

Calibration Flow, ml/s	Inspiratory		Expiratory
	Pam	Ppos	
Linear calibration			
1–6	6.8 ± 7.9†	9.2 ± 10.2*	3.1 ± 3.0*
4–10	6.7 ± 3.7*	8.0 ± 7.5*	2.7 ± 2.0*
8–12	9.9 ± 5.4*	9.9 ± 5.1*	4.0 ± 2.1*
1–12	7.0 ± 3.2*	8.2 ± 5.0*	2.8 ± 1.9*
Third-order polynomial calibration			
1–6	5.4 ± 8.6	16.2 ± 21.0	10.8 ± 18.2
4–10	1.3 ± 0.9	3.4 ± 4.6	1.1 ± 1.1
8–12	1.0 ± 0.7	1.1 ± 0.9	1.0 ± 0.8
1–12	0.9 ± 0.6	0.9 ± 0.7	0.8 ± 0.5

Values are means ± SD of absolute %errors obtained from 50 tests. Pam and Ppos, ambient and positive pressure, respectively. Calibration and test volume, 2.00 ml. *$P < 0.001$, tests at Ppos with mixed flow ranges. †$P < 0.05$, linear vs. polynomial calibration for same flow range.

condition. An evident flow dependence was observed for the linear calibration ($P < 0.001$ for both models). This dependence was absent in the data related to the third-order polynomial calibration.

Table 2 presents absolute error percents in the comparison of Pam and Ppos calibration conditions with both the normal- and low-compliance RS models. Fifty mixed-flow rate inspiratory injection tests for each compliance model at Ppos were done with the

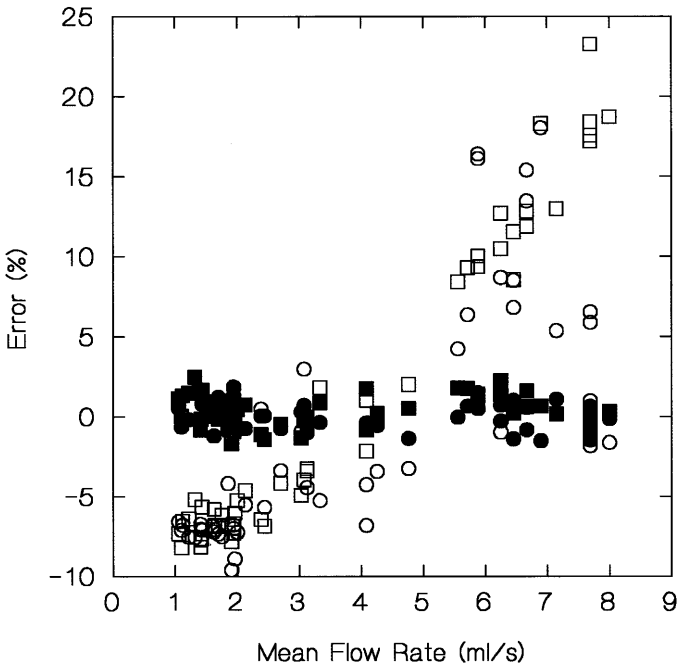

Fig. 5. Percent volume errors vs. mean flow rates for 50 tests at Ppos with normal (squares) or low (circles) compliance. Volumes were calculated by using linear (open symbols) or third-order polynomial (solid symbols) calibration. Calibrations were performed at Ppos by using mixed flow rates (1–12 ml/s). An evident dependence of error on flow with use of linear calibration is observed.

Table 2. *Errors in volume measurements during Ppos tests according to curve fitting and pressure condition used for calibration*

	Linear Calibration		Third-Order Polynomial Calibration	
Compliance	Pam	Ppos	Pam	Ppos
Normal	8.2 ± 4.9	8.2 ± 5.0	1.0 ± 0.8	0.9 ± 0.7
Low	8.6 ± 4.1	6.5 ± 4.0	4.5 ± 1.3	0.8 ± 0.5

Values are means ± SD of absolute %errors obtained from 50 tests for inspiratory injections by using calibrations based on linear and third-order polynomial fittings at mixed-flow ranges (1–12 ml/s) and performed with normal- or low-compliance model at Pam or Ppos. Calibration and test volume, 2.00 ml.

2.00-ml syringe. Notice that for low compliance, errors were higher for the Pam than for the Ppos calibration for both the linear (Pam = 8.6 ± 4.1 vs. Ppos = 6.5 ± 4.0, $P < 0.003$) and polynomial (Pam = 4.5 ± 1.3 vs. Ppos = 0.8 ± 0.5, $P < 0.001$) fittings. Third-order polynomial fitting lead to significantly lower error (0.8 ± 0.5) than linear fitting (6.5 ± 4.0) in the Ppos calibration condition ($P < 0.001$).

Figure 6 presents dependence of error on mean flow rate for 50 tests at Ppos for the low-compliance model. Calibrations were performed at Pam or Ppos and calculated by using linear or third-order polynomial fittings with use of different flow ranges (low, mean, or high). An evident dependence of error on flow rates is observed for the linear calibration.

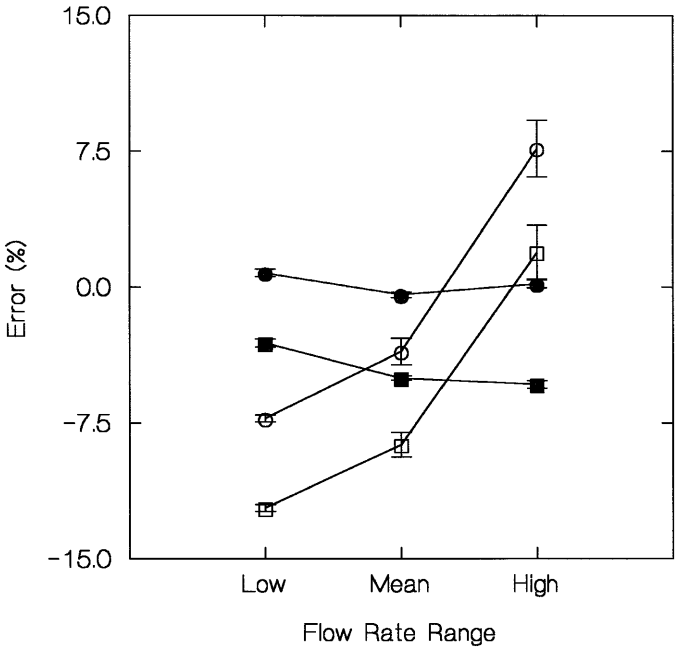

Fig. 6. Low-compliance model. Values are error percents ± SD of volume measurements for 50 tests at Ppos for linear (open symbols) or third-order polynomial (solid symbols) calibrations for Pam (squares) or Ppos (circles) at different flow ranges. Low, 1–6 ml/s; mean, 4–10 ml/s; high, 8–12 ml/s. Notice evident dependence on mean flow rate of linear calibration.

DISCUSSION

Pneumotachograph Design

The need for objective criteria for the design of pneumotachometers led to several works analyzing particular factors in the design of large pneumotachometers. In the case of pneumotachographs for small animals, basic work was performed by Mortola and Noworaj (13), who proposed four sets of fixed dimensions related to different animal sizes. The fact that such devices are often fashioned in the laboratory and that improvement of instrumentation characteristics, changes in the respiratory mechanics of the animal, and range of flows, volumes, and pressures to be investigated may involve the optimization of the pneumotachograph design lead to the development of the presented criteria. By using these criteria, objective adaptation of pneumotachometer design to improved electronics and/or experimental interests can be performed. The device built according to the criteria defined in this study performed adequately in the tests.

A narrow range for radii was determined in our specific set of conditions. Upper and lower limits were, respectively, due to measurability and minimal interference with pulmonary mechanics. Availability of more-sensitive transducers with low noise would allow for increase in the range toward large radii. Acceptance of higher load to respiratory mechanics, i.e., a larger percentage of respiratory resistance in the pneumotachograph, would increase the range, including small radii.

We have studied the influence of ΔP_{min} on the range of possible radii. With the consideration that ΔP_{min} is 0.1 Pa and by using L_{tot} of 60.0 mm and L (distance between pressure ports) of 15.0 mm, the range of possible radii was 0.874 mm < radius < 0.915 mm (chosen radius = 0.90 mm). If ΔP_{min} differs from 0.1 Pa, the dimensions of the pneumotachograph must be changed to allow for a new solution. The inequality 5 shows that if L is modified proportionally to ΔPmin, the inequality is unchanged. Thus a simple approach is to fix L_{tot} and change L to keep (P_{min}/L) = constant. For example, for ΔP_{min} of 0.2 Pa, considering that L_{tot} is 60 mm and L is 30 mm, the resulting radius range is the same as above.

Several simplifications were assumed in the definition of the presented criteria. One factor not included was the entrance effect. To have a fully developed flow, a given length should be provided before the differential pressure measurements. For laminar flow, the length to achieve a parabolic flow (L_p) is computed as $L_p/D = 0.058 \cdot Re$ and, thus $L_p > 0.058 \cdot Re \cdot D$ is the minimal length if a laminar flow is desired.

In our case of Re up to 543 and D of 1.80 mm, L_p results in a value of 5.7 cm. Thus such a factor could not be taken into account because it would involve, in cases of high Re, an extremely large dead space (a 3-fold increase in the pneumotachograph dead space in the present project). The consequence is that nonlinearities in the differential pressure-flow relationship are intro-

duced, and the proposed criteria must be regarded as the first approximation of the real situation because the parabolic flow profile, which is a necessary condition for *criteria 1–3*, is not necessarily attained. In a previous work (13) the entrance effect was suggested as playing a minimal role in pneumotachograph calibration, probably due to tubing upstream of the differential pressure measurement, which favors full development of flow combined with low Re. In the present case, the theoretical resistance computed from Poiseuille's law is 1.07×10^6 kg·m^{-4}·s and matches well the experimental value of 1.03×10^6 kg·m^{-4}·s obtained during inspiratory calibration with mixed flow rates under Pam conditions. This observation suggests that also in the present study the entrance effect has a small contribution in most of the tests. However, its role in the nonlinearities observed in the calibration curves at high flow rates (see Fig. 4) cannot be eliminated.

Physical Model

Physical models are devices used for evaluation of mechanical ventilators required by international standards (19). They also allow for in vitro testing of any device in the ventilatory experimental setup system in a condition close to real application. Previous work involving special setups in small animals by using controlled ventilation did not mention specific criteria for the design of the physical model and procedures to maintain isothermic conditions. Application of the pneumotachograph may occur in normal and diseased animals with a wide range of respiratory mechanics values. Thus a device that allows for evaluation in a specific interest range is important. The constructed model was compatible with design criteria and allowed for testing in pressure conditions from normal compliance to those compatible with rats in respiratory failure.

In the present study, isothermic conditions were kept through use of copper wire wool as a heat absorber. Pressures inside the RS model (for both normal and low compliances) were monitored during low- and high-flow injections of 2.00-ml volume. Only for the low-compliance model during high-flow injections, peak pressures exceeded plateau pressures (up to 3.8%). The ISO 5369/87 (19) standard requires that the difference between the peak and equilibrium values shall be $<5\%$ of the peak pressure. Thus isothermic conditions were met in the present case.

Calibration

The present results indicate that in a unicapillary pneumotachograph a nonlinear calibration provides significantly lower errors than a linear fitting, for both inspiratory and expiratory tests for all but one case (1–6 ml/s calibration range; see below). In addition to lower absolute error, nonlinear calibration error did not present dependence on mean flow rate in Pam and Ppos conditions (see Fig. 6). This is essentially because, provided an adequate flow range was used during calibration, the nonlinear curve can better adapt to pressure-flow relationships in the different flow ranges than can the linear fitting.

It must be underlined that use of nonlinear calibration involves previous knowledge of the flow range during an experiment. Table 1 and Fig. 4 show that extremely large errors may ensue if a nonlinear calibration is used out of the flow range for which it has been developed. In this case, a linear calibration would lead to smaller errors. It must be stressed that the error criterion is derived from volume measurements. Hence, much larger errors may be present in instantaneous flows values and any mechanical parameter derived from them.

Different functions might be used to fit the flow rate-differential pressure curve. Yeh et al. (22) used a conductance table to convert measured differential pressures into flow rates. Duvivier et al. (3) applied a nonlinear relationship with a threshold to correct flow rates from Fleisch pneumotachographs. Turner et al. (21) performed an evaluation of calibration polynomials for a 00 Fleisch pneumotachograph and concluded that third-order polynomials were adequate, with no increased accuracy with the use of a higher order. Giannella-Neto et al. (8) performed similar work addressing adult spirometry curves in a no. 3 Fleisch pneumotachograph and obtained results that indicated adequacy of use of third-order polynomials for pneumotachograph calibration. On the basis of these results, only a third-order polynomial was employed as a nonlinear fitting in the present work.

Small differences were observed in the comparison of Pam and Ppos calibrations for normal compliance. End-inspiratory pressures in the Ppos situation, equivalent to the experimental alveolar pressures, were in the range of 3.3 to 8.3 cmH_2O for injected volumes, equal to 2.00 and 5.00 ml, respectively. Larger errors were found when the same comparison was done in the case of a low-compliance model. In this situation, end-inspiratory pressures inside the model increased up to 27 cmH_2O. Figure 6 shows that in the presence of a low compliance, volume underestimation is observed for all flow rate ranges if a calibration done at Pam is used to measure volume during Ppos. The mean volume error was 4.49% (Table 2). Two main causes of this underestimation can be identified.

The first is the compression effect present during tests using the RS model, which leads to reduction of volume and volumetric flow rates and, thus, to underestimation of injected volumes. The maximal volume reduction for 27 cmH_2O would be 2.7%. Actually, because pressure increase is progressive, reduction in computed volume is lower and is ~1.4% of injected volume. Another consequence of compression is the increase in air density. As discussed in *Pneumotachograph Design*, flow is probably laminar during most of the cases. Thus change of density would play no role in determination of differential pressure. If turbulent flow is present, density becomes important and would lead to increased differential pressures. The second cause

for volume underestimation is the influence of the RS compliance on the flow rate to the pneumotachograph pressure connecting tubes. As described above, during inspiration, the tracheal pressure increases progressively up to 27 cmH_2O (low compliance). The pressure inside the connecting tubes increases in a similar fashion. As a consequence, a fraction of the volume goes to both tubes and does not enter the RS. This volume fraction depends on the relative compliances of the measuring setup and of the RS. We calculated the volume drain into the connecting tubes by using the model proposed by Farré et al. (5). For the RS with normal compliance, the pressure is very low. Therefore, the volume to the RS is roughly equal to the injected volume. However, for the low-compliance model, a reduction of 3.4% is calculated. One-half of the deviated volume goes to each connecting tube, and therefore the volume through the pneumotachograph is 98.3% of the injected volume and 101.7% of the volume effectively going into the RS. This volume can be roughly computed as the ratio between tubing and RS volumes and accounts, in the present case, for a volume underestimation of 1.7%.

Other factors might play a role in the changes of pressure-flow relationships in the present study. If isothermic conditions are not observed, temperature increases with a consequent tendency to volume expansion and pressure increase will be observed. As discussed in *Physical Model*, the experiments conformed to isothermic conditions. Temperature increase would also lead to rises in dynamic viscosity, which would cause an increase in the differential pressure readings. Observed errors were underestimations of expected values. Thus these factors were discarded as components of error.

The entrance effect could also be present in some situations, although it does not seem to be an important factor in most cases, as discussed above. If the pneumotachograph side ports were in the region of the entrance effects, differential pressures would be increased compared with differential pressures for the same flow during laminar conditions. Thus it would lead to overestimation, not underestimation, of volume and flow rates.

Another possible factor is the dynamic response related to the resistance device (20). The amplitude and phase changes due to different frequency components of the flow signal depend on the Womersley parameter: $\alpha = r \cdot (2 \cdot \pi \cdot f \cdot \rho/\eta)^{1/2}$, where f is frequency. The frequency components of the low- and high-flow injections in the present work were analyzed on their frequency spectrum by using a fast Fourier transform analysis. Ninety-five percent of energy was concentrated in frequencies below 2.9 Hz for low-flow injections and 7.4 Hz for high-flow injections. Computation of the Womersley parameter for 7.4 Hz provides an α value of 1.5, which leads to negligible amplitude changes and phase shift around 20°, suggesting a minimal role of dynamic response in the condition studied.

Frequency response of the measurement system was assessed on the basis of the model developed by Farré et al. (5). The pressure transducer, pneumotachograph, and all connecting tubes were considered and resistances, compliances, and inertances were estimated for each segment. The pressure transducer compliance was 0.002 ml/cmH_2O (5). Impedance of the physical model was included in both situations (normal and low compliance). The frequency response did not change significantly when the RS compliance was modified. For both situations, a resonance at 108 Hz was identified and the response was flat from 0 to 10 Hz. This frequency range included >95% of the energy of the manually driven flow signals used. The scope of the present work was directed to respiratory frequencies up to 1.5 Hz used to ventilate small animals. In this case, the present measurement system has a suitable frequency response. For the application devised in the study by Farré et al., this system may not be adequate. However, if the connecting tubes were smaller, the frequency response could be broadened.

Another important characteristic to be considered when pneumotachographs and differential pressure transducers are used is the common mode rejection ratio (CMRR). Peslin et al. (14) evaluated the effect of CMRR on the accuracy of respiratory input impedance measurements. Errors were larger when the resistance of the pneumotachograph was smaller (as in the present design) and the impedance of the subject was larger (one of our conditions, i.e., low compliance). These authors indicate the use of symmetrical pressure transducers and consider that the CMRR must be better than 40 dB at the highest work frequency (30 Hz).

We used a Celesco LCVR pressure transducer; the pressure connecting tubes were 10 cm long, and internal diameter was 0.4 cm. These tubes were as identical as possible, and we avoided any acute bends, to keep the internal diameter constant. We measured the CMRR for the Celesco LCVR pressure transducer. By using tubes 25 cm long, with an internal diameter of 0.4 cm, the CMRR was higher than 70 dB in the range between 2 and 32 Hz. Our results were similar to those of Duvivier et al. (4). Thus the Celesco LCVR pressure transducer with short tubes (10 cm) that were used presented a CMRR adequate for the intended measurements, especially in the frequency range under 10 Hz.

The pressure-wave propagation effect should be mentioned because it would lead to a decrease in differential pressure due to influence of the increased pressure on the mechanical model backward toward the side ports. However, the dimensions of the tubing setup are far too small to allow for this possible effect. This was corroborated experimentally by measuring changes in the pneumotachograph differential pressures when the expiratory limb was closed and an increase in pressure was caused in the model. Results showed negligible changes in the flow signal.

Thus, in a consideration of the possible sources of error, the composition of two effects, both caused by compression, was consistent with the observed error and results in 3.1% error, accounting for ~70% of the total obtained error.

Error percents were smaller when calibration was performed under the same pressure conditions as those in the test, i.e., Ppos conditions, than when Pam calibration was used. This was true for both linear and third-order polynomial fittings, the latter leading to lower absolute error percentages and less dependence on flow. Thus calibration in Ppos conditions results in important reduction of error in volume measurements and should be used when Ppos ventilation is involved, unless exclusively low pressures are expected. When the flow range to be used is known, nonlinear calibration allows for smaller flow and volume measurement errors.

In summary, we presented a set of objective criteria for design of unicapillary pneumotachographs. These criteria may help investigators to adjust instrument characteristics to their specific interests. A nonlinear calibration procedure based on a third-order polynomial was used to calibrate the pneumotachograph. This procedure lead to lower errors than the usual linear calibration and may be useful in flow and volume measurements using unicapillary pneumotachographs in small animals. When Ppos ventilation is involved, calibration in pressure conditions similar to experimental conditions should be used for reduction of flow and volume measurement error.

APPENDIX

Consider flow rate ($\dot{V}$) and pneumotachograph pressure drop (ΔP) related as

$$\dot{V} = f^n(\Delta P) \qquad (A1)$$

where f^n is a n-order polynomial function.

Once a syringe volume (Vs) is injected through the pneumotachograph and ΔP is digitized with a sampling period ΔT, Vs can be calculated as a discrete integral

$$Vs = \sum_j \dot{V}_j \cdot \Delta T = \sum_j f^n_j(\Delta P) \cdot \Delta T \qquad (A2)$$

$$\frac{Vs}{\Delta T} = a_1 \cdot \sum_j \Delta P_j + a_2 \cdot \sum_j \Delta P_j^2 + \ldots + a_n \cdot \sum_j \Delta P_j^n \qquad (A3)$$

where j is the sample number.

Each injection of Vs originates an equation similar to *Eq. A3*. Thus a set of m injections with different waveforms leads to a system of m-independent linear equations with the coefficients $a_1, a_2, \ldots, a_n$ as unknowns. In the case $m \geq n$, the system can readily be solved by minimizing the mean square error and the coefficients of the third-order calibration polynomial obtained.

The authors thank A. J. Xavier, C. F. M. Vasconcelos, L. T. Kagami, and R. M. Ichinose for technical support.

This work was partially supported by the Brazilian National Research Council (CNPq) and the Jose Bonifacio Foundation of the Federal University of Rio de Janeiro (UFRJ).

Present address of M. F. Vidal Melo: Dept. of Anesthesiology and Pain Management, Univ. of Texas Southwestern Medical Center, Dallas, TX 75235-9068.

Address for reprint requests: A. Giannella-Neto, Programa de Engenharia Biomedica, COPPE/UFRJ, Caixa Postal 68510, 21945-970 Rio de Janeiro RJ, Brazil (E-mail: agn@peb.ufrj.br).

Received 18 June 1997; accepted in final form 15 September 1997.

REFERENCES

1. **Brunner, J., H. Langenstein, and G. Wolff.** Direct accurate gas flow measurement in the patient: compensation for unavoidable error. *Med. Prog. Technol.* 9: 233–238, 1983.
2. **Diamond, L., and M. O'Donnell.** Pulmonary mechanics in normal rats. *J. Appl. Physiol.* 43: 942–948, 1977.
3. **Duvivier, C., R. Peslin, and C. Gallina.** An incremental method to assess the linearity of gas flowmeters: application to Fleisch pneumotachographs. *Eur. Respir. J.* 1: 661–665, 1988.
4. **Duvivier, C., M. Rotger, J. Felicio da Silva, R. Peslin, and D. Navajas.** Static and dynamic performances of variable reluctance and piezoresistive pressure transducers for forced oscillation measurements. *Eur. Respir. J.* 1: 146–150, 1991.
5. **Farré, R., R. Peslin, D. Navajas, C. Gallina, and B. Suki.** Analysis of the dynamic characteristics of pressure transducers for studying respiratory mechanics at high frequencies. *Med. Biol. Eng. Comput.* 27: 531–537, 1989.
6. **Finucane, K. E., B. A. Egan, and S. V. Dawson.** Linearity and frequency response of pneumotachographs. *J. Appl. Physiol.* 32: 121–126, 1972.
7. **Gelfand, R., C. J. Lambertsen, R. E. Peterson, and A. Slater.** Pneumotachograph for flow and volume measurement in normal and dense atmospheres. *J. Appl. Physiol.* 41: 120–124, 1976.
8. **Giannella-Neto, A., M. J. O. Vale, and M. F. Vidal Melo.** Accurate calibration of pneumotachographs using a syringe and polynomial curve fitting (Abstract). In: *Proceedings of the Eleventh Annual Conference of IEEE/EMBS Paris France 1992.* Piscataway, NJ: IEEE, 1992, vol. 2, p. 693–694.
9. **Glass, M. L., S. C. Wood, and K. Johansen.** The application of pneumotachography on small unrestrained animals. *Comp. Biochem. Physiol. A Physiol.* 59A: 425–427, 1978.
10. **Lai, Y. L., and J. Hildebrandt.** Respiratory mechanics in the anesthetized rat. *J. Appl. Physiol.* 45: 255–260, 1978.
11. **Marano, G.** Airflow measurement in small animals. *Lab. Anim.* 28: 239–243, 1994.
12. **Mauderly, J. L.** Measurement of respiration and respiratory responses during inhalation exposures. *J. Am. Coll. Toxicol.* 9: 397–405, 1990.
13. **Mortola, J. P., and A. Noworaj.** Two-sidearm tracheal cannula for respiratory airflow measurements in small animals. *J. Appl. Physiol.* 55: 250–253, 1983.
14. **Peslin, R., P. Jardin, C. Duvivier, and P. Begin.** In-phase rejection requirements for measuring respiratory input impedance. *J. Appl. Physiol.* 56: 804–809, 1984.
15. **Pols, W. M.** Pneumotachography. *Acta Anaesth. Scandinav.* 171–179, 1962.
16. **Scheid, P.** Respiratory mass spectrometry. In: *Measurement in Clinical Respiratory Physiology*, edited by G. Lazlo and M. Sudlow. London: Academic, 1983, p. 131–165.
17. **Schuessler, G. B., and J. H. T. Bates.** A computer-controlled research ventilator for small animals: design and evaluation. *IEEE Trans. Biomed. Eng.* 42: 860–866, 1995.
18. **Schuessler, T. F., J. H. T. Bates, and G. N. Maksym.** Estimating tracheal flow in small animals (Abstract). In: *Proceedings of the Fifteenth Annual Conference of IEEE/EMBS San Diego California 1993.* Piscataway, NJ: IEEE, 1993, vol. 1, p. 560–561.
19. **Technical Committee ISO/TC 121.** *Breathing Machines for Medical Use—Lung Ventilators (ISO 5369).* Geneva, Switzerland: International Organization for Standardization, 1987.
20. **Turner, M. J., I. M. MacLeod, and A. D. Rothberg.** Lumped parameter approximation for the prediction of the dynamic response of the fleisch pneumotacograph. *Med. Biol. Eng. Comput.* 26: 443–448, 1988.
21. **Turner, M. J., I. M. MacLeod, and A. D. Rothberg.** Calibration of Fleisch and screen pneumotachographs for use with various oxygen concentrations. *Med. Biol. Eng. Comput.* 28: 200–204, 1990.
22. **Yeh, M. P., R. M. Gardner, T. D. Adams, and F. G. Yanowitz.** Computerized determination of pneumotachometer characteristics using a calibrated syringe. *J. Appl. Physiol.* 53: 280–285, 1982.